A Journal of the Gesellschaft Deutscher Chemiker
Angewandte
GDCh
International Edition
Chemie
www.angewandte.org

Accepted Article

Title: Unveiling the Intrinsic Catalytic Activities of Single Gold Nanoparticle-based Enzyme Mimetics

Authors: Wei Ma, Mahmoud Elsayed Hafez, Hui Ma, and Yi-Tao Long

To be cited as: *Angew. Chem. Int. Ed.* 10.1002/anie.201901384
Angew. Chem. 10.1002/ange.201901384

Link to VoR: http://dx.doi.org/10.1002/anie.201901384
http://dx.doi.org/10.1002/ange.201901384

WILEY-VCH

10.1002/anie.201901384

WILEY-VCH

Unveiling the Intrinsic Catalytic Activities of Single Gold Nanoparticle-based Enzyme Mimetics

Mahmoud Elsayed Hafez, Hui Ma, Wei Ma* and Yi-Tao Long*

Abstract: *Gold nanoparticles (AuNPs) have been demonstrated to serve as the effective nanomaterial-based enzyme mimetics (nanozymes) for a number of enzymatic reactions under mild conditions. Intrigued by single NP collision electrochemical measurements, we investigated the intrinsic catalytic activities of single AuNPs and Ag-Au nanohybrids as glucose oxidase and peroxidase-like mimetics, respectively. Our electrochemical results showed that significantly high turnover number of nanozymes was obtained from individual catalytic events compared with the results from the classical, ensemble-averaged measurements. We ascribed that the unusual enhancement of catalytic activity of single nanozyme came from the high accessible surface area of monodispersed NPs and the high activities of carbon-supported NP during single particle collision at a carbon ultramicroelectrode. This work introduced a new method for precise characterization of the intrinsic catalytic activities of nanozymes, giving further insights to design high-efficient nanomaterial catalysts.*

Nanomaterials exhibit the unique prosperities owing to their physical size, tunable properties and large accessible inorganic surfaces.[1–3] With the merging of nanotechnology with biology, nanomaterials have been developed to possess enzyme-like catalytic activities to imitate the essential principles of natural enzymes.[4–7] Unlike nature enzymes, NPs as artificial nanozymes possess several advantages, such as low cost and facile synthesis, recycling and recovery, robustness to harsh environments, long time storage, large surface area, as well as tunability in catalytic activities.[4,7–9] Therefore, nanozymes are considered as the promising candidates of natural enzymes to treat enzyme deficiency-related conditions.[10-13]

AuNPs, one of the most widely studied NPs, have been regarded as highly inert nanomaterial.[14] Recently, they have been found to exhibit surprising enzyme-mimic activities with different surface modifications.[5,8,15–22] For instance, citrate-capped AuNPs show the remarkable glucose oxidase (GOx) mimetic activities.[18–20] Furthermore, the change of capping molecule or the adsorption of metal ions (Hg^{2+}, Bi^{3+}, Ag^{+}, Pb^{2+}, etc.) on AuNPs surface could alter their enzyme-like activities, i.e. switch their activity to peroxidase nanomimetics.[19,23–25] Because the catalytic activity of NPs is highly dependent on their shape, size and surface modification, the correlation between structure and performance are of great utility in the design of more efficient catalytic systems.[23,26] Despite ongoing progress in the development of these artificial catalytic systems, the intrinsic structure−activity relationships remain challenging due to the average effect of traditional ensemble measurements.[19,20,27] Additionally, the catalytic activities of various nanomaterials are not systematically compared due to the unfair performance evaluation testing, resulting from different mass loading of nanomaterials on electrode and different preparation methods of the electrode.[28-31] This point needs to be addressed under the same conditions for screening the optimal nanocatalysts.

Single NP collision electrochemistry have attracted increasing interests over the past several decades motivated by the unique electrochemical behaviors of single NPs during their collision processes at an ultramicroelectrode (UME) surface, unveiling the intrinsic properties masked in the ensemble-averaged measurements.[32–37] With the rapid development, stochastic collision electrochemical measurements have been applied from electrocatalytic amplification and direct electrochemical stripping of individual metal NPs to soft particles and blocking detection of biologically relevant samples.[38,39] Recently, Compton's group have been devoted to assessing the electrocatalytic activity of single NPs by stochastic collision measurements.[40,41] It was demonstrated to give important and complementary insights to the conventional analysis usually performed on the ensemble measurements, opening up a new possibility of testing the nanomaterials performance in conditions that are more realistically close to the ones when the NPs are dispersed in the environment. Herein, we aimed to report a high-resolution electrochemical detection of enzyme-like activity of single nanozyme at which AuNPs catalyzed glucose oxidation, meanwhile Ag-Au nanohybrids catalyzed hydrogen peroxide oxidation (Figure 1). We successfully monitored the anodic current transients produced in a catalytic oxidation reaction from glucose to gluconic acid by a single AuNP as GOx mimetics when it collided with an UME. Since the substrate can be selected to have a high concentration and a high diffusion coefficient, large amplification allowed a measurable current in a rapid electrocatalytic reaction of single NP collision events. Moreover, citrate capped AuNPs modified with Ag^{+} ions as Ag-Au nanohybrids caused different enzymatic activities that switched on the peroxidase mimics activity and totally blocked the oxidase mimics activity due to the changes of surface

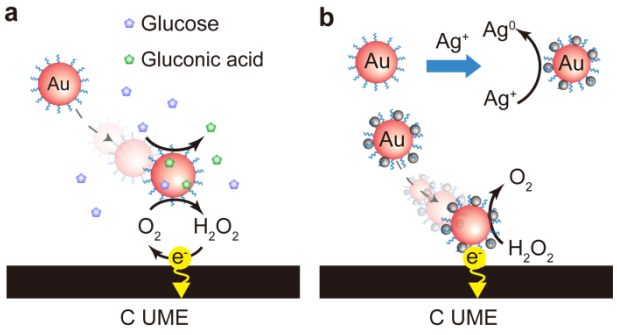

Figure 1. Scheme illustrates the electrochemical detection of catalytic current of a single nanozyme during a collision at a CUME surface. a) GOx-like activity of single citrate-AuNPs. b) An enhanced peroxidase mimetics activity is activated by adding Ag^{+} ions to citrate-AuNPs.

[*] M.E. Hafez, H. Ma, Dr. W. Ma and Prof. Y.-T. Long
Key Laboratory for Advanced Materials, School of Chemistry & Molecular Engineering, East China University of Science and Technology,
130 Meilong Road, Shanghai, 200237, P. R. China
E-mail: weima@ecust.edu.cn
ytlong@ecust.edu.cn

Supporting information for this article is given via a link at the end of the document.

properties of AuNPs.

Typically, small sized citrate-capped AuNPs possess high activity of GOx.[19] Comparative studies of UV-vis spectra and transmission electron microscopy (TEM) image showed that AuNPs had a narrow size distribution with an average diameter of 16 ± 2 nm, and the as-prepared particles were dispersed homogeneously (Figure S1). Moreover, the colorimetric results and UV-vis spectra demonstrated citrate-capped AuNPs catalytically oxidized glucose in the presence of O_2 (Figure S2), generating H_2O_2 and gluconic acid by Equation 1:

$$glucose + O_2 \xrightarrow{AuNPs} \text{gluconic } acid + H_2O_2 \qquad (1)$$

In this study, carbon fiber UME with diameter of 6.8 μm (CUME, Figure S3) was used as an inert electrode surface to investigate the enzyme-like activities of single AuNPs. To guarantee that the collision events occurred at individual NPs level, we selected the concentration of monodispersed AuNPs solution to be 200 pM. The applied potential used in the acquisition of the collision experiments was optimized to + 600 mV vs Ag/AgCl wire (Figures S4). Before addition of AuNPs, we observed a smooth curve in 20 mM PBS solution at pH 7.4 containing 10 mM glucose (Figure S5). After the injections of AuNPs, significant current transients were observed for the catalytic oxidation of glucose for individual AuNPs upon collision at CUME surface (Figure 2a). In a typical collision event, a characteristic single peak appeared with duration of 0.21 ± 0.02 ms (Figure 2b) and current amplitude of 14.4 ± 0.1 pA (bottom black ordinate in Figure 2c). During the collision process, AuNPs probably collided elastically and receded from the electrode surface, thus producing the spike-like current signals. To confirm that these transient signals were due to the catalytic oxidation of glucose on AuNPs, a control experiment was performed under the identical condition, but without glucose. Current transients were toally disappeared (Figure S6a), suggesting glucose acts as the efficient reaction substrates in our GOx mimetic system. Moreover, no current transient was observed in glucose solution containing AuNPs after approximately 5 min of bubbling argon gas prior to making measurements while the electrochemical cell was kept under argon atmosphere throughout the experiment (Figure S6b). This means that the collision of 16 nm AuNPs at the CUME cannot directly electrocatalyze the oxidation of glucose in the absence of O_2 in a neutral solution. We speculated the current spike was due to the oxidation of H_2O_2 as individual AuNPs landed on the CUME at +600 mV vs Ag/AgCl, resulting in the regeneration of O_2 for the next catalytic oxidation (Figure 1a). Therefore, the experimentally measured current spike was not only a reflection of the diffusion of individual AuNPs to the surface of CUME, but also a reflection of the locally generated H_2O_2 at a single AuNP.

Considering two electrons are needed for the oxidation of one molecule of glucose, we can calculate the turnover number (TON) for catalytic glucose oxidation of a single AuNP per single collision event at CUME from the measured transients by Equation 2:

$$\text{TON} = \frac{Q}{2e} \qquad (2)$$

where Q is the integrated charge quantity of single AuNP collision event and e is the elementary charge. We found that the measured integrated charge of the representative individual current transients was 1.6 ± 0.1 fC (bottom black ordinate in Figure 2d). This allowed us to calculate a total TON of (4.9 ± 0.1) × 10^3 for a typical single-particle collision event, revealing the intrinsic electron transfer number of a single AuNP as GOx mimetics. Figure 2d represented a fluctuation distribution of single nanozyme kinetics, implying that the catalytic ability of AuNPs toward glucose oxidation has certain heterogeneity at the single NP level or alternatively that individual AuNPs for the same batch sample have particle-to-particle size variation.

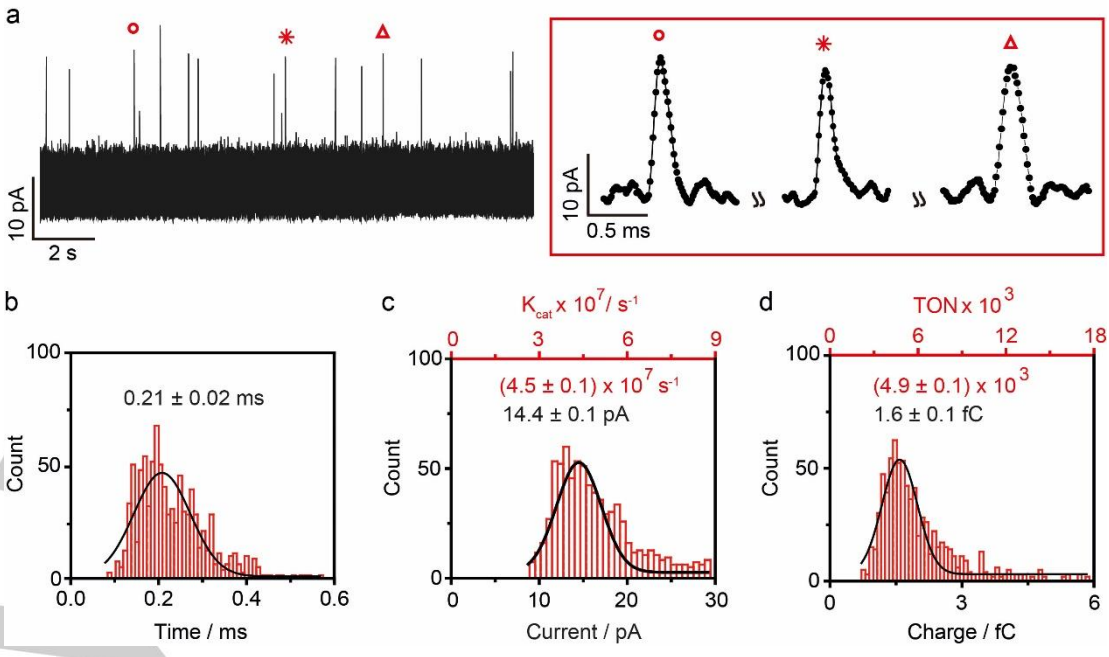

Figure 2. Electrochemical response of individual AuNPs nanozymes as GOx mimetics for catalytic oxidation of glucose. a) Amperometric current-time curve of 200 pM AuNPs upon collision at a CUME in 20 mM PBS of pH 7.4 containing 10 mM glucose at +600 mV vs Ag/AgCl wire. The red rectangle is a zoom-in of the representative current traces of single AuNP nanozymes with same legend. Histograms showing the distributions of the duration time b), the peak current height (bottom black ordinate) and k_{Cat} (top red ordinate) c), and the integrated charge (bottom black ordinate) and TON (top red ordinate) d) of individual AuNPs collision events. Black curves show Gaussian fits. Data were obtained from the chronoamperometry curves from a large population of catalytic oxidation events of individual AuNPs (more than 1000 events).

Notably, our method has allowed measurement of the distribution and fluctuations of nanozyme properties unattainable from ensemble averaging data. This is the major point of interest of single entity electrochemistry that lies in the difference between single nanozymes and ensembles.[42,43] To further estimate the catalytic rate of a single AuNP nanozyme, we used the measured peak current, I, for the maximum turnover numbers (k_{Cat}) by Equation 3:

$$k_{cat} = \frac{I}{2e} \qquad (3)$$

The observed current amplitude, 14.4 ± 0.1 pA, gave a k_{Cat} estimation for GOx-like AuNPs to be (4.5 ± 0.1) x 10^7 s^{-1} (top red ordinate in Figure 2c). In this work, single AuNPs exhibited hundreds- or even thousands-fold enhancement of GOx-like activity compared with the previously obtained results based on the averaged ensemble measurements,[20,44–47] which was consistent with the catalytic kinetics of a free diffusing single enzyme with high TON using single entity electrochemical measurements.[29,42,43] Significantly enhanced catalytic activity can be best explained by considering the high accessible surface area of monodispersed AuNPs in our measurement.[40,41] Moreover, carbon as the support can develop different interactions with AuNPs during their collision processes at a CUME surface, thus modifying both the electronic and structural properties of AuNPs.[48] Additionally, the unique carbon structure of CUME can trap the reactant glucose, which facilitates the contact between glucose molecules and AuNPs on its surface.[49] In fact, the abundant active oxygen species existing on the carbon surface also promote glucose oxidation.[50,51] Our results further demonstrated that the performance-enhancement of nanomaterial catalyst depended on the accessibility of active sites and the support of choice for enhanced charge transfer.

Moreover, the potential-dependent GOx-like enzymatic activities of AuNPs were observed in stochastic collision measurements. In principle, the catalytic activity of AuNPs agrees with the concept that only exposed atoms are catalytically active. Based on this fact, the theoretical k_{Cat} value of AuNPs should be similar under different applied potentials, considering similar catalytic surface area for the same batch sample (as derived by TEM). However, the current amplitude, the collision frequency, and integrated charge increased as the applied potential increased from +400 mV to +800 mV vs Ag/AgCl (Figure S7). Under the potential of +800 mV vs Ag/AgCl, the TON and k_{Cat} for GOx-like enzymatic activity of a single AuNP were (7.2 ± 0.1) × 10^3 and (6.3 ± 0.1) x 10^7 s^{-1}, respectively, which were 1.5 times higher than that of obtained at +600 mV vs Ag/AgCl (Figure S8). We proposed that our chronoamperometric measurements of individual AuNPs were performed at room temperature, while GOx works at 37 ºC and AuNPs as GOx mimetics work at 34 ºC in the colorimetric experiment (Figure S2b).[18,42] Thus applying an anodic potential works as a driving force, the same role like temperature incubation, to overcome the energy barrier for glucose oxidation on the surface of AuNPs. At the more positive potential, the stronger driving force was applied for the oxidation of H_2O_2 at CUME, resulting in the faster reaction kinetics. That is, the potential-dependent GOx-like enzymatic activities of AuNPs could further reflect the efficiency of H_2O_2 capture. However, the dwell time of individual AuNPs on the surface of CUME cannot be affected by the applied potential.

By modeling single AuNP as a spherical electrode, for a mass transport controlled process, the expected peak current on a single AuNP at the CUME from the oxidation of glucose can be estimated based on the following Equation 4:

$$i_{\lim} = 4\pi \ln(2)\, nFDCr_{NP} \qquad (4)$$

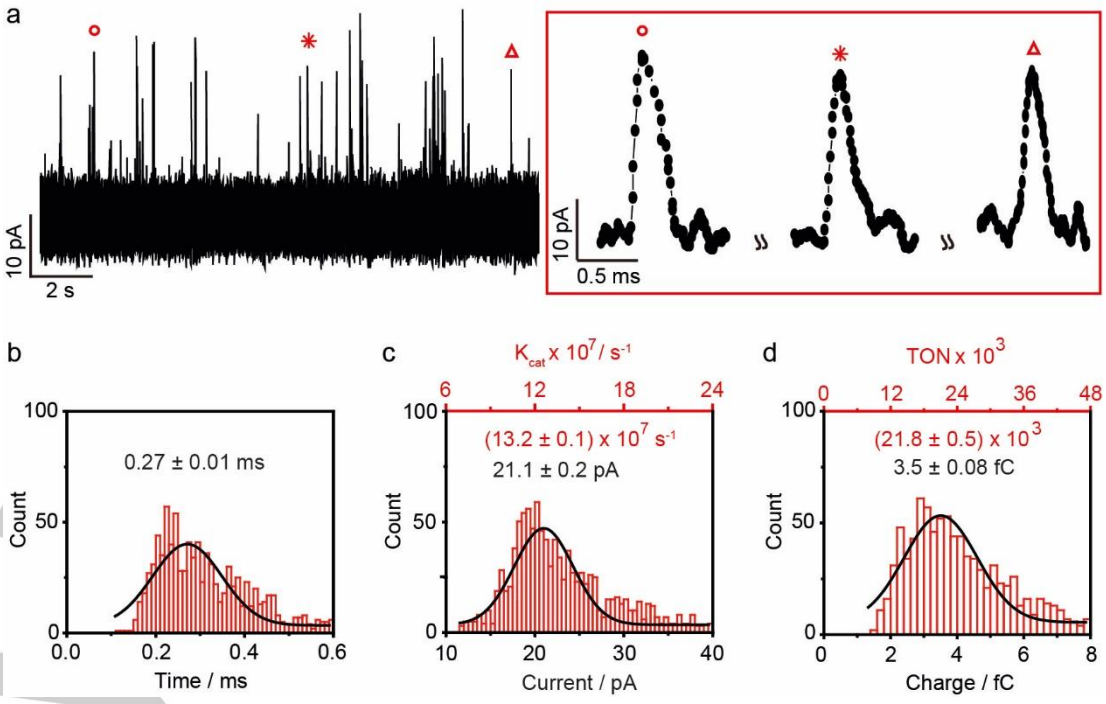

Figure 3. Electrochemical response of individual Ag-Au nanohybrids as peroxidase mimetics for catalytic oxidation of H_2O_2. a) Amperometric current-time curve of 200 pM Ag-Au nanohybrids upon collision at a CUME in 20 mM acetate buffer of pH 4.1 containing 3 mM H_2O_2 at +300 mV vs Ag/AgCl wire. The red rectangle is a zoom-in of the representative current traces of single Ag-Au nanohybrids. Histograms showing the distributions of duration time b), the peak current height (bottom black ordinate) and k_{Cat} (top red ordinate) c), and the integrated charge (bottom black ordinate) and TON (top red ordinate) d) of individual Ag-Au nanohybrids collision events. Black curves show Gaussian fits. Data were obtained from the chronoamperometry curves from a large population of catalytic oxidation events of individual AuNPs (more than 1000 events).

where i_{lim} is the diffusion-limited current, n is the electron transfer number (2 for glucose oxidation), F is the Faraday constant (96485 C/mol), D is the diffusion coefficient of glucose (6.8×10^{-6} cm^2/s),[52] C is the concentration of glucose and r_{NP} is the AuNP radius. Therefore, for 10 mM glucose, the theoretical diffusion-limited current at a AuNP nanosphere electrode with radius of 8 nm can be estimated to be 9.14×10^{-11} A. However, the experimentally measured oxidative currents of 10 mM glucose (14.4 ± 0.1 pA) were much smaller than the hypothetical diffusion-limited values, evidencing that glucose oxidation on AuNPs surface is surface reaction rate-limited processes, rather than being under mass transport control. This would suggest our GOx-like catalytic reaction at AuNPs was unperturbed from the concentration gradient of glucose, further confirming the anodic current spikes from the oxidation of H_2O_2 on the CUME.

To clearly clarify the origin of the catalytic activities of single AuNPs, we further investigated the horseradish peroxidase (HRP) mimics activities of citrate-capped AuNPs.[5,25] A mixture of AuNP nanozymes and glucose at 34 ºC was incubated for 30 min to allow GOx mimics reaction and H_2O_2 production. Then, 1 mM ABTS solution was injected to the mixture while measuring the HRP mimics activities. No significant color was observed instantly after injection of ABTS solution (Figure S9) compared to the instant color obtained by the injection of both HRP and ABTS (Figure S2b, red), suggesting a negligible instant HRP-like activity of citrate-capped AuNPs at room temperature. Therefore, all results demonstrated that our collision electrochemical measurements unveiled the intrinsic GOx-like activities of AuNPs due to the H_2O_2 capture as the product of AuNPs nanozyme, not the other electrocatalytic performances.

Interestingly, the various enzyme-like activities of AuNPs can be obtained *via* the surface modification.[53] Generally, GOx mimics activities of AuNPs are affected in the presence of metal ions.[5] For instance, the reduction of Ag^+ ions on the surface of citrate-capped AuNPs can change the surface properties of NPs[53] and thus dramatically stimulate the enzymatic activity of peroxidase[54] followed by Equation (5):

$$H_2O_2 \xrightarrow{Ag-Au\ NPs} H_2O + \frac{1}{2} O_2 \qquad (5)$$

Indeed, the colorimetric results and UV-vis spectra showed a remarkable peroxidase-like activity upon addition of Ag^+ ions to citrate-capped AuNPs solution in presence of H_2O_2 and TMB (Figure S10). To make a comparable electrochemical analysis, the concentration of NPs was still selected to be 200 pM. To confirm the role of Ag modification, we investigated the chronoamperometric curve of individual AuNPs at +300 mV vs Ag/AgCl wire in a solution containing 3 mM H_2O_2 in 20 mM acetate buffer of pH 4.1 (Figure S11). Negligible current transients were observed, indicating citrate-capped AuNPs cannot electrocatalyze the oxidation of H_2O_2 under our experimental conditions. After 5 min incubation of AuNPs solution with 20 μM Ag^+ ions at room temperature, high-resolution TEM images and energy diffraction X-ray spectra demonstrated that the Ag-Au nanohybrids were obtained (Fig. S12). As expected, significant spikes were observed in the amperometric current–time curves due to the switch "on" of the peroxidase catalytic reaction on the surface of Ag-Au nanohybrids (Figure 3a). Individual collision events of modified AuNPs in this case afforded a symmetrical parabolic current trace, yielding a duration of 0.27 ± 0.01 ms (Figure 3b) and a current amplitude of 21.1 ± 0.2 pA (bottom black ordinate in Figure 3c). Notably, the duration of peroxidase mimics activity was longer than that obtained from GOx mimics activity. This observation could be ascribed that Ag-Au nanohybrids had a rough surface (Fig. S12d) to enhance their adsorption properties toward the electrode surface, thus elongating the dwell time of particles on CUME. Accordingly, both current height and integrated charge revealed the corresponding k_{Cat} and TON of Ag-Au nanohybrids to be (13.2 ± 0.1) x 10^7 s^{-1} and (21.8 ± 0.5) x 10^3 for H_2O_2 oxidation, respectively (top red ordinates in Figure 3c and 3d). Similarly, Ag-Au nanozymes showed a remarkable peroxidase mimics activity with high maximum turnover number over ensemble measurement (Figure 3c).[16] Moreover, Ag-Au nanohybrids hindered the GOx mimics activity, which was evidenced by the smooth amperometric curve in a performed control experiment containing Ag-Au nanohybrids in glucose solution at +600 mV vs Ag/AgCl (Figure S13).

In summary, we have demonstrated the possibility to real-time monitor the enzyme-like catalytic behaviors of single NP as nanozyme mimetics. Based on the high-resolution electrochemical measurements, our results can be used for quantifying the intrinsic enzymatic activities of a single AuNP and Ag-Au nanohybrid as glucose oxidase and peroxidase-like mimetics, respectively. Unlike the average traditional ensemble measurements, our methods not only illustrated the hyperactivity of Au and Ag-Au nanozyme mimetics at the carbon-support but also opened a way to study the catalytic activity of nanozymes at single NP level. In this respect, this work provides new insights to design high performance biomimetic nanocatalysts by coupling the intrinsic catalytic activities of nanozyme mimetics.

Acknowledgements

This research was supported by the National Natural Science Foundation of China (21775043, 214210047), the Program of Introducing Talents of Discipline to Universities (B16017), Innovation Program of Shanghai Municipal Education Commission (2017-01-07-00-02-E00023), and the Fundamental Research Funds for the Central Universities (222201718001, 222201717003).

Conflict of interest

The authors declare no conflict of interest.

Keywords: nanozyme • single nanoparticle • intrinsic activity • electrocatalysis • enzyme mimetics

[1] H. Yang, J. Zha, P. Zhang, Y. Xiong, L. Su, F. Ye, *RSC Adv.* **2016**, *6*, 66963–66970.

[2] C. Chen, S. Fan, C. Li, Y. Chong, X. Tian, J. Zheng, P. P. Fu, X. Jiang, W. G. Wamer, J. Yin, *J. Mater. Chem. B* **2016**, *4*, 7895–7901.

[3] Z. Xiang, H. Deng, P. Peljo, Z. Fu, S. Wang, D. Mandler, G. Sun, Z.

Liang, *Angew. Chem. Int. Ed.* **2018**, *57*, 3464–3468.
[4] Y. Lin, J. Ren, X. Qu, *Acc. Chem. Res.* **2014**, *47*, 1097–1105.
[5] Y. Lin, J. Ren, X. Qu, *Adv. Mater.* **2014**, *26*, 4200–4217.
[6] N. Sui, F. Liu, K. Wang, F. Xie, L. Wang, J. Tang, M. Liu, W. W. Yu, *Sensors Actuators B Chem.* **2017**, *252*, 1010–1015.
[7] H. Wei, E. Wang, *Chem. Soc. Rev.* **2013**, *42*, 6060–6093.
[8] R. Singh, R. Belgamwar, M. Dhiman, V. Polshettiwar, *J. Mater. Chem. B* **2018**, *6*, 1600–1604.
[9] A. Dalui, B. Pradhan, U. Thupakula, A. H. Khan, G. S. Kumar, T. Ghosh, B. Satpati, S. Acharya, *Nanoscale* **2015**, *7*, 9062–9074.
[10] E. Priyadarshini, K. Rawat, *J. Mater. Chem. B* **2017**, *5*, 5425–5432.
[11] L. Gao, J. Zhuang, L. Nie, J. Zhang, Y. Zhang, N. Gu, T. Wang, J. Feng, D. Yang, S. Perrett, X. Yan, *Nat. Nanotechnol.* **2007**, *2*, 577–583.
[12] J. Yu, D. Ma, L. Mei, Q. Gao, W. Yin, X. Zhang, L. Yan, Z. Gu, X. Ma, Y. Zhao, *J. Mater. Chem. B* **2018**, *6*, 487–498.
[13] H. Jia, D. Yang, X. Han, J. Cai, H. Liu, W. He, *Nanoscale* **2016**, *8*, 5938–5945.
[14] A. Gerber, M. Bundschuh, D. Klingelhofer, D. A. Groneberg, *J. Occup. Med. Toxicol.* **2013**, *8*, 32.
[15] H. Liao, G. Liu, Y. Liu, R. Li, W. Fu, L. Hu, *Chem. Commun.* **2017**, *53*, 10160–10163.
[16] J. Liu, X. Hu, S. Hou, T. Wen, W. Liu, X. Zhu, J. J. Yin, X. Wu, *Sensors Actuators B Chem.* **2012**, 708–714.
[17] W. He, Y. Liu, J. Yuan, J. J. Yin, X. Wu, X. Hu, K. Zhang, J. Liu, C. Chen, Y. Ji, Y. Guo, *Biomaterials* **2011**, *32*, 1139–1147.
[18] X. Zheng, Q. Liu, C. Jing, Y. Li, D. Li, W. Luo, Y. Wen, Y. He, Q. Huang, Y. T. Long, C. Fan, *Angew. Chem. Int. Ed.* **2011**, *50*, 11994–11998.
[19] W. Luo, C. Zhu, S. Su, D. Li, Y. He, Q. Huang, C. Fan, *ACS Nano* **2010**, *4*, 7451–7458.
[20] P. Beltrame, M. Comotti, C. Della Pina, M. Rossi, *Appl. Catal. A Gen.* **2006**, *297*, 1–7.
[21] P. Pengo, S. Polizzi, L. Pasquato, P. Scrimin, *J. Am. Chem. Soc.* **2005**, *127*, 1616–1617.
[22] M. Comotti, C. Della Pina, R. Matarrese, M. Rossi, *Angew. Chem. Int. Ed.* **2004**, *43*, 5812–5815.
[23] Y. Lin, Z. Li, Z. Chen, J. Ren, X. Qu, *Biomaterials* **2013**, *34*, 2600–2610.
[24] Y. Jv, B. Li, R. Cao, *Chem. Commun.* **2010**, *46*, 8017–8019.
[25] Y. J. Long, Y. F. Li, Y. Liu, J. J. Zheng, J. Tang, C. Z. Huang, *Chem. Commun.* **2011**, *47*, 11939–11941.
[26] C. Jiang, J. Zhu, Z. Li, J. Luo, J. Wang, Y. Sun, *RSC Adv.* **2017**, *7*, 44463–44469.
[27] X. Zhou, W. Xu, G. Liu, D. Panda, P. Chen, *J. Am. Chem. Soc.* **2010**, *132*, 138–146.
[28] X. Xiao, F. R. F. Fan, J. Zhou, A. J. Bard, *J. Am. Chem. Soc.* **2008**, *130*, 16669–16677.
[29] A. N. Sekretaryova, M. Y. Vagin, A. P. F. Turner, M. Eriksson, *J. Am. Chem. Soc.* **2016**, *138*, 2504–2507.
[30] X. Xiao, A. J. Bard, *J. Am. Chem. Soc.* **2007**, *129*, 9610–9612.
[31] H. Zhou, F. R. F. Fan, A. J. Bard, *J. Phys. Chem. Lett.* **2010**, *1*, 2671–2674.
[32] J. H. Park, A. Boika, H. S. Park, H. C. Lee, A. J. Bard, *J. Phys. Chem. C* **2013**, *117*, 6651–6657.
[33] W. Ma, H. Ma, J. F. Chen, Y. Y. Peng, Z. Y. Yang, H. F. Wang, Y. L. Ying, H. Tian, Y. T. Long, *Chem. Sci.* **2017**, *8*, 1854–1861.
[34] L. Chen, E. E. L. Tanner, C. Lin, R. G. Compton, *Chem. Sci.* **2017**, *9*, 152–159.
[35] Y. Y. Peng, R. C. Qian, M. E. Hafez, Y. T. Long, *ChemElectroChem* **2017**, *4*, 977–985.
[36] G. Zampardi, J. Thöming, H. Naatz, H. M. Amin, S. Pokhrel, L. Mädler, R. G. Compton, *Small* **2018**, *14*, 1801765 (1-9).
[37] E. Kätelhön, E. E. L. Tanner, C. Batchelor-Mcauley, R. G. Compton, *Electrochim. Acta* **2016**, *199*, 297–304.
[38] J. E. Dick, A. T. Hilterbrand, A. Boika, J. W. Upton, A. J. Bard, *Proc. Natl. Acad. Sci.* **2015**, *112*, 5303–5308.
[39] W. Cheng, R. G. Compton, *Angew. Chem. Int. Ed.* **2016**, *55*, 2545–2549.
[40] X. Li, H. Hodson, C. Batchelor-Mcauley, L. Shao, R. G. Compton, *ACS Catal.* **2016**, *6*, 7118–7124.
[41] X. Jiao, C. Lin, N. P. Young, C. Batchelor-McAuley, R. G. Compton, *J. Phys. Chem. C* **2016**, *120*, 13148-13158.
[42] C. Lin, L. Sepunaru, E. Kätelhön, R. G. Compton, *J. Phys. Chem. Lett.* **2018**, *9*, 2814–2817.
[43] C. Lin, E. Kätelhön, L. Sepunaru, R. G. Compton, *Chem. Sci.* **2017**, *8*, 6423–6432.
[44] Z. Tao, R. A. Raffel, A. K. Souid, J. Goodisman, *Biophys. J.* **2009**, *96*, 2977–88.
[45] P. Beltrame, M. Comotti, C. Della Pina, M. Rossi, *J. Catal.* **2004**, *228*, 282–287.
[46] Q. H. Gibson, B. E. P. Swoboda, V. Massey, *J Biol Chem* **1964**, *239*, 3927–3934.
[47] R. Venugopal, B. A. Saville, *Can. J. Chem. Eng.* **1993**, *71*, 917–924.
[48] Villa , M. Schiavoni, L. Prati, *Catal. Sci. Technol.* **2012**, *2*, 673-682.
[49] T. Ishida, N. Kinoshita, H. Okatsu, T. Akita, T. Takei, M. Haruta, *Angew. Chem. Int. Ed.* **2008**, *47*, 9265–9268.
[50] A. Corma, H. Garcia, *Chem. Soc. Rev.* **2008**, *37*, 2096–2126.
[51] C. Ma, W. Xue, J. Li, W. Xing, Z. Hao, *Green Chem.* **2013**, *15*, 1035–1041.
[52] T. Zhang, H. H. P. Fang, *Environ. Technol.* **2005**, *26*, 155–160.
[53] C. I. Wang, W. T. Chen, H. T. Chang, *Anal. Chem.* **2012**, *84*, 9706–9712.
[54] C. W. Lien, Y. C. Chen, H. T. Chang, C. C. Huang, *Nanoscale* **2013**, *5*, 8227–8234.

10.1002/anie.201901384

WILEY-VCH

Entry for the Table of Contents

COMMUNICATION

Intrinsic catalytic activity of single nanozyme: Our method could be used for quantifying the intrinsic catalytic activities of single nanozymes using stochastic collision electrochemistry, providing new insights for designing high-efficient nanomaterial catalysts.

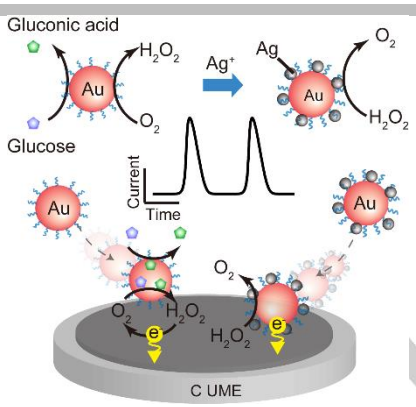

Mahmoud Elsayed Hafez, Hui Ma, Wei Ma and Yi-Tao Long**

Page No. – Page No.

Unveiling the Intrinsic Catalytic Activities of Single Gold Nanoparticle-based Enzyme Mimetics